

1 Analytical model for two-dimensional pollutant transport in defective 2 GM/GCL/SL composite liners

3 Shan Zhao ^{a, b}, Botao Sun^a, Xinjia Su^a

4 ^a*College of Ocean Science and Engineering, Shanghai Maritime University, Shanghai 201306,*
5 *China*

6 ^b*College of Civil Engineering, Tongji University, Shanghai 200092, China*

7 **Abstract:** This study presents an analytical model for two-dimensional pollutant transport in a
8 three-layer composite liner system, comprising a geomembrane (GM), a geosynthetic clay liner
9 (GCL), and a soil liner (SL), with a focus on the impact of defects in the GM. By utilizing Laplace
10 and Fourier transforms, the model derives pollutant concentration distributions, incorporating
11 processes such as convection, diffusion, adsorption, and degradation. Validation against COMSOL
12 simulations demonstrated the model's accuracy. The findings reveal that traditional models
13 significantly underestimate longitudinal pollutant migration and overestimate lateral migration.
14 These insights emphasize the necessity for advanced analytical methods in order to enhance the
15 design and effectiveness of landfill liner systems.

16 **Keywords:** Analytical model; Two-dimensional; Defective composite liner; Landfill;
17 Geomembrane

18 1. Introduction

19 Landfills serve as a critical component of waste management systems, particularly for the
20 disposal of municipal solid wastes and industrial by-products (Gómez-García et al., 2021; Ghosh et
21 al., 2023; Ling et al. 2024; Nanda and Berruti, 2021; Qian et al., 2024; Woodman et al., 2017).
22 However, one of the major concerns associated with landfills is the potential for leachate migration
23 from the waste into the surrounding environment (Sobral et al., 2024; Wu et al., 2021; Zhang et al.,
24 2021). To mitigate this, composite liner systems are widely used (Abiriga et al., 2020; Shu et al.,

25 [2019](#); [Teng et al., 2021](#); [Wijekoon et al., 2022](#)). These systems typically consist of a geomembrane
26 (GM), a geosynthetic clay liner (GCL), and a soil layer (SL), working in unison to contain leachate
27 and prevent contaminants from seeping into groundwater and the surrounding soil ([Trauger and](#)
28 [Tewes, 2020](#)). Despite the effectiveness of these composite liners under ideal conditions, defects in
29 the liners can occur due to various factors such as construction issues, material degradation, or
30 external stresses ([Touze-Foltz et al., 2021](#); [Rowe and Hamdan, 2022](#); [Rowe et al., 2023](#); [Sun et al.,](#)
31 [2019](#)). Such defects may compromise the integrity of the liners and result in pollutant leakage.
32 Understanding the transport mechanisms of pollutants in these compromised systems is therefore
33 crucial for assessing environmental risks and improving landfill designs.

34 The study of pollutant transport through landfill liners has been an area of considerable
35 research over the past few decades. Numerous models have been developed to describe the transport
36 of contaminants through liner systems. Traditionally, one-dimensional models have been used,
37 focusing on vertical transport through the layers. For instance, [Xie et al. \(2013\)](#) developed a 1D
38 model using Laplace transform to describe the diffusion of organic pollutants through a three-layer
39 composite liner, providing an analytical solution as an alternative to numerical models. Similarly,
40 [Yu et al. \(2018\)](#) proposed a migration and transformation model for pollutants in 1D layered porous
41 media, comprehensively considering the effects of adsorption and biodegradation. Other researchers,
42 such as [Pu et al. \(2019\)](#) and [Feng et al. \(2019b\)](#), developed models that considered the diffusion and
43 transient migration of pollutants, respectively, further refining the predictions of pollutant behavior
44 in composite liners.

45 Although these models have provided valuable insights into pollutant transport mechanisms,
46 they often simplify the complex, multi-dimensional nature of real-world landfill scenarios. In reality,

47 pollutant migration in defective liners is not confined to the vertical direction; it can also occur
48 laterally, necessitating more sophisticated two-dimensional (2D) models. Former advancements
49 have attempted to address this complexity. For instance, [Dominijanni and Manassero \(2021\)](#)
50 provides analytical solutions for pollutant concentrations in the vertical and horizontal directions,
51 aiding in the evaluation of the equivalence and effectiveness of composite liners. [Rouholahnejad](#)
52 [and Sadrnejad \(2009\)](#) used 2D advection-diffusion-linear sorption with first order decay equation
53 to assess leachate migration from the landfill to groundwater, the transport of pollutants after the
54 leachate enters the surface was further clarified.

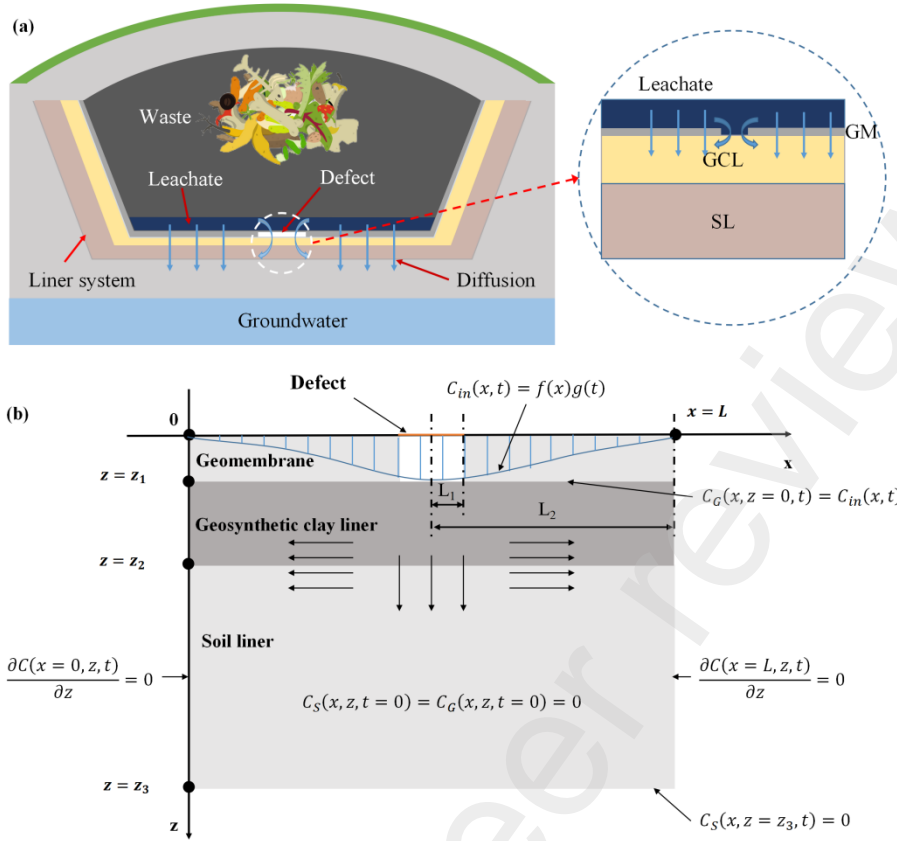
55 Despite the progress made in modeling pollutant transport through composite liners, several
56 critical challenges remain. A major issue is the limited consideration of defects in the GM layer.
57 These defects can drastically alter the containment efficacy of liner systems, leading to significant
58 deviations from the predictions made by models that assume intact conditions. For instance, [Xie et](#)
59 [al. \(2010\)](#) modeled the steady-state transport of pollutants through a defective GM and demonstrated
60 that defects could substantially affect pollutant migration patterns, especially when varying GM
61 conditions are considered. Moreover, current models often do not fully account for the coupled
62 physical processes—such as diffusion, advection, retardation, and degradation—that occur within
63 the liner system. These processes interact in complex and nonlinear ways, particularly in the
64 presence of defects, making it challenging to accurately predict pollutant transport. The need for
65 more precise initial concentration distributions, as highlighted by [Xie et al. \(2014\)](#) and [Sun et al.](#)
66 [\(2022\)](#), further complicates the modeling of defective systems. Additionally, there remains a
67 significant gap in understanding how defects impact the transport of different types of pollutants,
68 such as heavy metals and organic compounds, which behave differently within composite liners.

69 Given these challenges, this study aims to fill critical gaps in the understanding of pollutant
70 transport in defective GM/GCL/SL composite liners. The primary objective is to present an
71 innovative 2D analytical model that comprehensively examines convection, diffusion, adsorption,
72 and degradation under defect conditions, supported by precise mathematical derivations and
73 numerical validation. The findings are expected to enhance the effectiveness of containment
74 strategies, ultimately leading to better protection of the environment from landfill-related pollution.

75 **2. Mathematical model**

76 *2.1 Basic assumptions*

77 As shown in [Fig.1a](#), the composite liner system considered in this study comprises a GM, GCL,
78 and SL ([Fig.1b](#)). The GM layer is assumed to be in a defective state, allowing direct contact with
79 the leachate. In the context of the model, z_1 represents the thickness of the GM, z_2 represents the
80 combined thickness of the GM and GCL, z_3 represents the combined thickness of the GM, GCL and
81 SL. L_1 represents the width of the leak, and L_2 represents the length from the leak to the next leak
82 in the GM. The model is based on the following assumptions: (1) The flow of leachate within the
83 liner is steady-state and obeys Darcy's law; (2) Migration of metal pollutants through the non-
84 defective GM is neglected; (3) Both the GCL and SL are assumed to be fully saturated and have
85 uniform properties ([Wu et al., 2015](#)); (4) The effects of convection, diffusion, adsorption, and
86 degradation are considered.



87

88 **Fig. 1.** The migration of leachate through the composite liner system:(a) schematic diagram; (b)
89 mathematical model.

90 *2.2 Governing equations and boundary conditions*

91 Based on the above assumptions, the two-dimensional transport of pollutants in the
92 GM/GCL/SL composite liner can be described by the equations of convection, diffusion, adsorption,
93 and degradation .

94 For the GCL:

$$95 \quad R_{d,G} \frac{\partial C_G}{\partial t} = D_{x,G} \frac{\partial^2 C_G}{\partial x^2} + D_{z,G} \frac{\partial^2 C_G}{\partial z^2} - v_G \frac{\partial C_G}{\partial z} - \lambda_G C_G \quad (1)$$

96 For the SL:

$$97 \quad R_{d,S} \frac{\partial C_S}{\partial t} = D_{x,S} \frac{\partial^2 C_S}{\partial x^2} + D_{z,S} \frac{\partial^2 C_S}{\partial z^2} - v_S \frac{\partial C_S}{\partial z} - \lambda_S C_S \quad (2)$$

98 where $C_i(i=G,S)$ represents the concentration of pollutants in the liner layer, which is a function
99 of position and time; $R_{d,i}$ represents the adsorption retardation factor of the i -th layer of liner; $D_{x,i}$

100 and $D_{z,i}$ represent the diffusion coefficient in the x and z directions of the i -th layer, respectively; v_i
 101 is the convection coefficient in the liner layer; and λ_i represents the degradation constant of organic
 102 pollutants.

103 The expressions for the adsorption retardation factor (R_d) and degradation coefficient (λ) are
 104 respectively:

$$105 \quad R_d = 1 + \frac{\rho K_d}{n} \quad (3)$$

$$106 \quad \lambda = \frac{\ln 2}{t_{1/2}} \quad (4)$$

107 Where ρ is the density of the liner, K_d is the distribution coefficient of the liner and $t_{1/2}$ is
 108 the half-life of an organic pollutants.

109 Assuming the liner system has not been contaminated at the outset, the initial conditions of the
 110 liner system are :

$$111 \quad C_S(x,z,t=0) = C_G(x,z,t=0) = 0 \quad (5)$$

112 $C_S(x,z,t)$ represents the concentration of SL, $C_G(x,z,t)$ represents the concentration of
 113 GCL. The boundary conditions for the entrance of the GM defect can be represented by a
 114 concentration function in terms of width (x) and time (t):

$$115 \quad C_M(x,z=0,t) = C_{in}(x,t) \quad (6)$$

116 $C_M(x,z,t)$ represents the concentration of GM, the function $C_{in}(x,t)$ represents the
 117 concentration of the pollutant source, which is the product of a function $f(x)$ related to the width
 118 and a function $g(t)$ related to time.

$$119 \quad C_{in}(x,t) = f(x)g(t) \quad (7)$$

120 The lower boundary of the composite liner is assumed to be a semi-infinite boundary.

$$121 \quad C_S(x,z=z_3,t) = 0 \quad (8)$$

122 The left and right boundary condition of the model can be written as:

123
$$\frac{\partial C(x=0,z,t)}{\partial z} = 0 \quad (9)$$

124
$$\frac{\partial C(x=L,z,t)}{\partial z} = 0 \quad (10)$$

125 The concentration and flux at the interface between GCL and SL are equal, with expressions
126 as follows:

127
$$C_G(x,z=z_1,t) = C_S(x,z=z_1,t) \quad (11)$$

128
$$-n_G D_G \frac{\partial C_G(x,z=z_1,t)}{\partial z} + n_G v_G C_G(x,z=z_1,t) = -n_S D_S \frac{\partial C_S(x,z=z_1,t)}{\partial z} + n_S v_S C_S(x,z=z_1,t) \quad (12)$$

129 Where z_1 represents the thickness of GCL, $n_i (i = G, S)$ represents the porosity of the i -th layer.

130 2.3 Analytical solution

131 By applying the Laplace transform to the governing equations, the following equations can be
132 obtained:

133
$$\bar{g}(s) = L(g(t)) = \int_0^{+\infty} g(t) e^{-St} dt \quad (13)$$

134 For the GCL:

135
$$D_{x,G} \frac{\partial^2 \bar{C}_G(x,z,s)}{\partial x^2} + D_{z,G} \frac{\partial^2 \bar{C}_G(x,z,s)}{\partial z^2} - v_G \frac{\partial \bar{C}_G(x,z,s)}{\partial z} - (R_{d,G} s + \lambda_G) \bar{C}_G(x,z,s) = 0 \quad (14)$$

136 For the SL:

137
$$D_{x,S} \frac{\partial^2 \bar{C}_S(x,z,s)}{\partial x^2} + D_{z,S} \frac{\partial^2 \bar{C}_S(x,z,s)}{\partial z^2} - v_S \frac{\partial \bar{C}_S(x,z,s)}{\partial z} - (R_{d,S} s + \lambda_S) \bar{C}_S(x,z,s) = 0 \quad (15)$$

138 Where $\bar{C}_G(x,z,s)$ and $\bar{C}_S(x,z,s)$ are the form of $C_G(x,z,t)$ and $C_S(x,z,t)$, respectively. s is
139 the Laplace transform parameter.

140 Applying the Fourier series transform to equation yields the following equation:

141
$$\hat{F}(k) = F_c[f(z)] = \frac{2}{H} \int_0^H f(z) \cos\left(\frac{k\pi z}{H}\right) dz \quad (16)$$

142 For the GCL:

143
$$D_{z,G} \frac{\partial^2 \bar{C}_G(k,z,s)}{\partial z^2} - v_G \frac{\partial \bar{C}_G(k,z,s)}{\partial z} - \left(R_{d,G}S + \lambda_G + \frac{k^2 \pi^2 D_{z,G}}{H^2} \right) \hat{C}_G(k,z,s) = 0 \quad (17)$$

144 For the SL:

145
$$D_{z,S} \frac{\partial^2 \bar{C}_S(k,z,s)}{\partial z^2} - v_S \frac{\partial \bar{C}_S(k,z,s)}{\partial z} - \left(R_{d,S}S + \lambda_S + \frac{k^2 \pi^2 D_{z,S}}{H^2} \right) \hat{C}_S(k,z,s) = 0 \quad (18)$$

146 Where $\bar{C}_G(k,z,s)$ and $\bar{C}_S(k,z,s)$ are the form of $\bar{C}_G(x,z,s)$ and $\bar{C}_S(x,z,s)$ after Fourier series
147 transform, respectively. k is the corresponding transform parameter.

148 Applying the same transform to both the boundary conditions and the equations, we obtain the
149 following equation:

150 For the boundary conditions:

151
$$C_G(k,z=0,s) = C_{in}(k,s) = f(k)g(s) \quad (19)$$

152
$$C_S(k,z=z_3,s) = 0 \quad (20)$$

153 For the equivalent interfacial concentration:

154
$$\hat{C}_G(k,z=z_1,s) = \hat{C}_S(k,z=z_1,s) \quad (21)$$

155 For the equivalent interfacial flux:

156
$$n_G v_G \frac{\partial \hat{C}_G(k,z=z_1,s)}{\partial z} = n_S v_S \frac{\partial \hat{C}_S(k,z=z_1,s)}{\partial z} \quad (22)$$

157 The homogeneous general solution of the concentration function can be written as:

158
$$\hat{C}_i(k,z,s) = M_i e^{\alpha_i z} + N_i e^{\beta_i z} \quad (23)$$

159 α_i, β_i can be expressed as:

160
$$\alpha_i, \beta_i = \frac{\left\{ v \pm \sqrt{v_i^2 + 4D_{z,i} \left(R_{d,i}S + \lambda_i + \frac{k^2 \pi^2 D_{z,i}}{H^2} \right)} \right\}}{2D_{z,i}} \quad (24)$$

161 The matrix equation:

162
$$\begin{bmatrix} M_S \\ N_S \end{bmatrix} = A \begin{bmatrix} M_G \\ N_G \end{bmatrix} \quad (25)$$

163 Expression for coefficient A :

164
$$A = \frac{1}{\alpha_S - \beta_S} \begin{bmatrix} (\gamma\alpha_G - \beta_S)e^{(\alpha_G - \alpha_S)z_1} & (\gamma\beta_G - \beta_S)e^{(\beta_G - \alpha_S)z_1} \\ (\alpha_S - \gamma\alpha_G)e^{(\alpha_G - \beta_S)z_1} & (\alpha_S - \gamma\beta_G)e^{(\beta_G - \beta_S)z_1} \end{bmatrix} \quad (26)$$

165 Expression for coefficient γ :

166
$$\gamma = \frac{n_G D_{z,G}}{n_S D_{z,S}} \quad (27)$$

167 Express coefficient A in matrix form:

168
$$A = \begin{bmatrix} A_{11} & A_{12} \\ A_{21} & A_{22} \end{bmatrix} \quad (28)$$

169 Translation of the concentration expression when z is zero:

170
$$\hat{C}_G(k, z = 0, s) = M_G + N_G = \hat{f}(k)\bar{g}(s) \quad (29)$$

171 Translation of the concentration expression when z equals z_2 :

172
$$\hat{C}_S(k, z = z_2, s) = M_S e^{\alpha_S z} + N_S e^{\beta_S z} = 0 \quad (30)$$

173 The correlation between concentration expression and matrix form:

174
$$\begin{bmatrix} M_G \\ N_G \end{bmatrix} = \begin{bmatrix} \frac{-A_{12}e^{\alpha_S z_2} - A_{22}e^{\beta_S z_2}}{A_{11}e^{\alpha_S z_2} - A_{12}e^{\alpha_S z_2} + A_{21}e^{\beta_S z_2} - A_{22}e^{\beta_S z_2}} \\ \frac{A_{11}e^{\alpha_S z_2} + A_{21}e^{\beta_S z_2}}{A_{11}e^{\alpha_S z_2} - A_{12}e^{\alpha_S z_2} + A_{21}e^{\beta_S z_2} - A_{22}e^{\beta_S z_2}} \end{bmatrix} \hat{f}(k)\bar{g}(s) \quad (31)$$

175 Applying the inverse transform to the equation, the solution for the original problem is finally

176 obtained:

177 For the GCL :

178
$$\bar{C}_G(x, z, s) = \frac{1}{2}(M_G e^{\alpha_G(k=0,s)z} + N_G e^{\beta_G(k=0,s)z}) + \sum_{k=1}^{+\infty} (M_G e^{\alpha_G z} + N_G e^{\beta_G z}) \cos\left(\frac{k\pi x}{H}\right) \quad (32)$$

179 For the SL :

180
$$\bar{C}_S(x, z, s) = \frac{1}{2}(M_S e^{\alpha_S(k=0,s)z} + N_S e^{\beta_S(k=0,s)z}) + \sum_{k=1}^{+\infty} (M_S e^{\alpha_S z} + N_S e^{\beta_S z}) \cos\left(\frac{k\pi x}{H}\right) \quad (33)$$

181 3. Model verification

182 To validate the effectiveness and reasonableness of the analytical solution in this study, an

183 analytical solution for solute transport in double-layered finite porous media was chosen as a

184 benchmark. The liner system model used in this study consists of a 1.5 mm GM, a 1 cm GCL, and

185 a 75 cm SL. The analytical solution was validated using the one-dimensional analytical solution
 186 provided by [Feng et al. \(2019b\)](#). In this study, the water head was set at 0.3 m, and the other
 187 coefficients are provided in the [Table 1](#) below.

188 The results, as shown in [Fig.2](#), indicate that at the two-year mark, the pollutant concentration
 189 calculated by the model shows some differences from the data in the reference literature at distances
 190 further from the GCL. This discrepancy is attributed to the consideration of pollutant degradation
 191 within the liner in this study, resulting in lower pollutant concentrations at greater distances
 192 compared to the reference literature.

193 To further validate the model's accuracy in two dimensions, COMSOL Multiphysics 6.0 was
 194 used to compare the concentrations of pollutants after one year and two years. The results
 195 demonstrate a high degree of consistency between the COMSOL model and the analytical solution
 196 utilized in this study, providing robust validation for these research outcomes. The parameters used
 197 are as follows:([Ding et al., 2020](#); [Feng et al., 2019b](#); [Foose et al., 2002](#); [Xie et al., 2023](#); [Xie et al.,](#)
 198 [2014](#))

199 **Table 1**
 200 Parameters used in this study

Parameter	Pollutants	GM	GCL	SL
Thickness, L (m)	–	0.0015	0.01	0.75
Porosity, n	–	–	0.7	0.3
Dry density, ρ_d (g/cm ³)	–	–	0.79	1.62
Hydraulic conductivity, k (m/s)	–	–	0.5×10^{-10}	1×10^{-7}
	–	3×10^{-13}	3×10^{-10}	8×10^{-10}
Effective diffusion coefficient, D (m ² /s)	Zn ²⁺	6×10^{-15}	7.15×10^{-10}	8.9×10^{-10}
	TOL	3×10^{-13}	3×10^{-10}	8×10^{-10}
Distribution coefficient, K_d (mL/g)	–	0	0	0
Partition coefficient, K_g	–	100	–	–

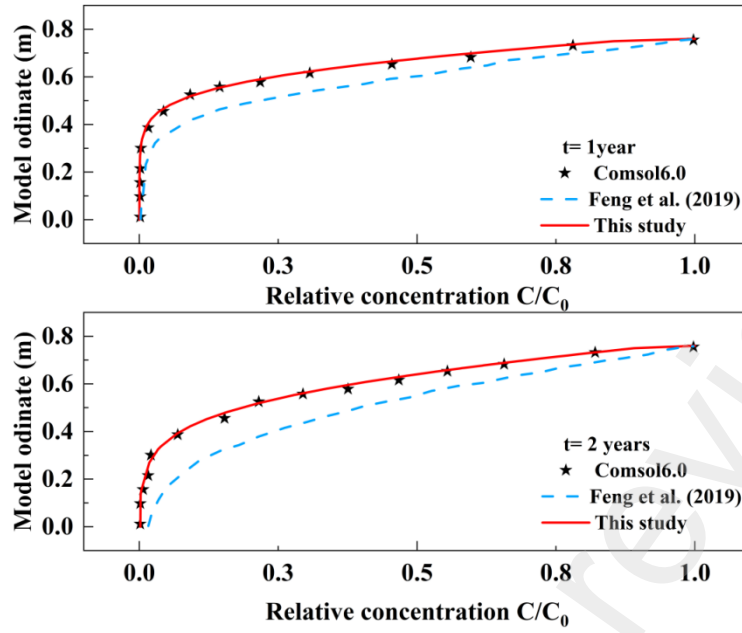


Fig. 2. Comparison of the solution in this study with the existing solution.

4. Uneven distribution of pollutant concentrations at the liner leak points

Damage to the GM in the liner system results in a non-uniform distribution of pollutant concentrations during the subsequent transport through the liner. As shown in Fig.3, the diffusion coefficient of heavy metal pollutants in the GM is significantly smaller than that in the defective areas. Therefore, this study employs distinct concentration functions for heavy metal pollutants and organic pollutants. Specifically, for heavy metal ion pollutants, this study uses the concentration function related to the width and length of the leak as proposed by Sun et al. (2022).

$$C|_{z=0} = \begin{cases} 1, & 0 \leq x \leq \lambda \\ \zeta \frac{\partial C}{\partial z}|_{z=0} + 1, & \lambda \leq x \leq 1 \end{cases} \quad (34)$$

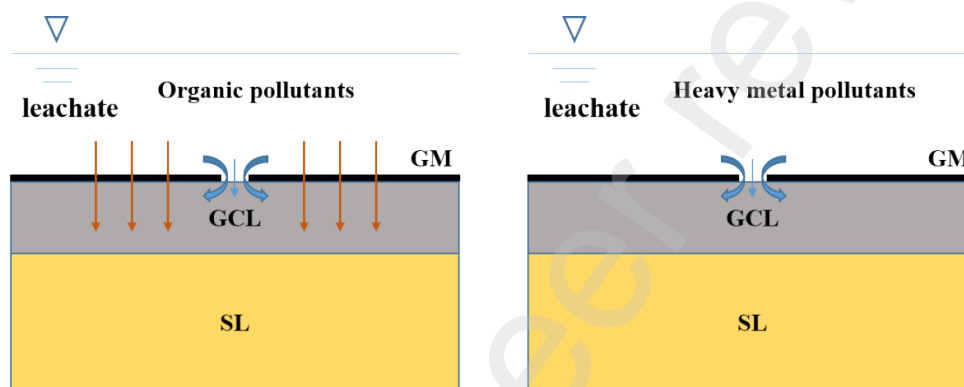
Here, $\lambda = L_1/L_2$, coefficient $\zeta = \frac{D_{S,z}L_G}{S_g D_G L_S}$, $D_{S,z}$ represents the vertical diffusion coefficient in the soil liner, L_G represents thickness of GM, S_g represents partition coefficient, D_G is diffusion coefficient of the GM, L_S is the thickness of SL. Since heavy metal ions cannot degrade in the liner, the control equation can be simplified accordingly:

$$R_{d,i} \frac{\partial C_i}{\partial t} = D_{x,i} \frac{\partial^2 C_i}{\partial x^2} + D_{z,i} \frac{\partial^2 C_i}{\partial z^2} - v_i \frac{\partial C_i}{\partial z} \quad (35)$$

216 For organic pollutants, the concentration distribution can be more accurately described using the
 217 standard Gaussian function, as mentioned by Ding et al. (2020), to provide a more precise
 218 description of the concentration distribution.

$$219 \quad C = C_{in,max} \times \exp(- (x - \mu) / 2\sigma^2) \quad (36)$$

220 Where $C_{in,max}$ represents the largest concentration of the pollutant source, μ represents the
 221 abscissa of $C_{in,max}$, σ represents the distribution range of the high concentration.



222

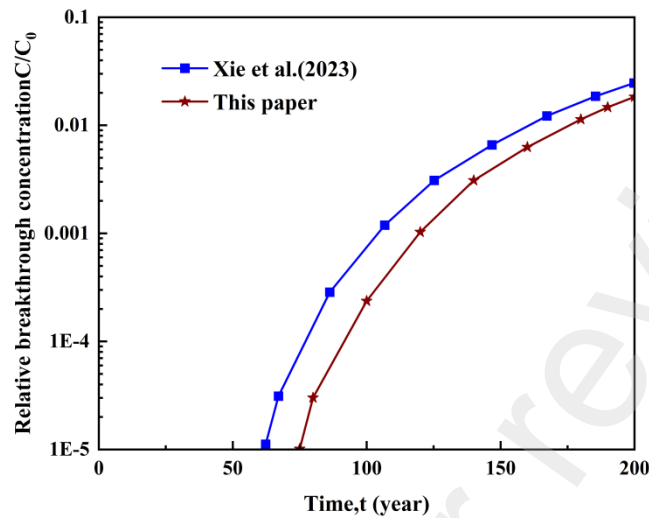
223 **Fig. 3.** Transportation process of organic pollutants and heavy metal pollutant

224 **5. Pollution prevention performance of composite liner systems**

225 *5.1 Heavy metal ion zinc (Zn^{2+})*

226 Zn^{2+} is common heavy metal pollutant found in leachate. Therefore, this heavy metal ion was
 227 selected for analysis. The only significant pathway for contaminant transport is through defects in
 228 the geomembrane (Foose et al., 2002). Using Eq.(34) as the initial concentration distribution
 229 function for Zn^{2+} . Fig.4 presents the breakthrough concentration of Zn^{2+} within the liner system over
 230 different time intervals. As time elapses, the breakthrough concentration of Zn^{2+} in the liner
 231 increases. However, the results of this paper are consistently slightly less than the results of Xie et
 232 al. (2023). This is caused by the differences in concentration distribution functions. As time

233 increases, the deviation in breakthrough concentration gradually decreases. This indicates that this
234 function can be used to describe the transport of heavy metal ions.



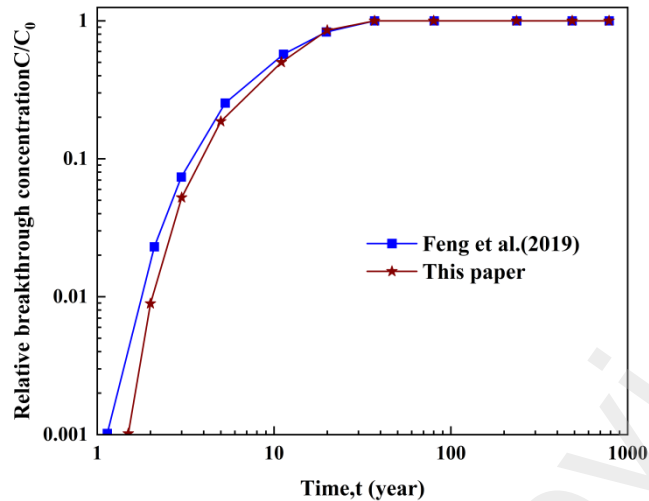
235

236 **Fig. 4.** Comparison of breakthrough concentration of Zn^{2+} under different time factors

237 5.2 Organic pollutant TOL

238 Leachate typically contains a substantial quantity of organic pollutants. If these organic
239 pollutants were to leak through the GM and migrate through the composite liner system, they could
240 cause significant damage to the soil and groundwater. Using Eq.(36) as the initial concentration
241 distribution function, therefore, this study focuses on TOL as a representative organic pollutant to
242 investigate its migration within the composite liner system, as illustrated in Fig.5.

243 Organic pollutants, such as TOL, exhibit a higher diffusion capacity within the liner compared
244 to heavy metal pollutants, making them more likely to penetrate the GM. Due to its faster diffusion
245 rate within the liner system, the breakthrough time of TOL less than the time of Zn^{2+} . When the
246 migration time is short, there is a subtle difference between this study and Feng et al. (2019b).
247 However, after 20 years, the breakthrough concentration of the two become basically consistent.
248 These findings underscore that that function can be used to describe the transport of organic
249 pollutants.



250

251 **Fig. 5.** Comparison of breakthrough concentration of TOL under different time factors

252 6. Model parameter analysis

253 For the GM/GCL/SL composite liner system, this study analyzed the effects of changes in SL
 254 thickness, diffusion coefficients of GCL and SL, convection coefficients, and adsorption hindrance
 255 factors on the migration of pollutants within the liner layer. The parameters of the reference model
 256 are provided in [Table 1](#). When one parameter is changed, the other parameters are kept constant.

257 6.1 SL thickness

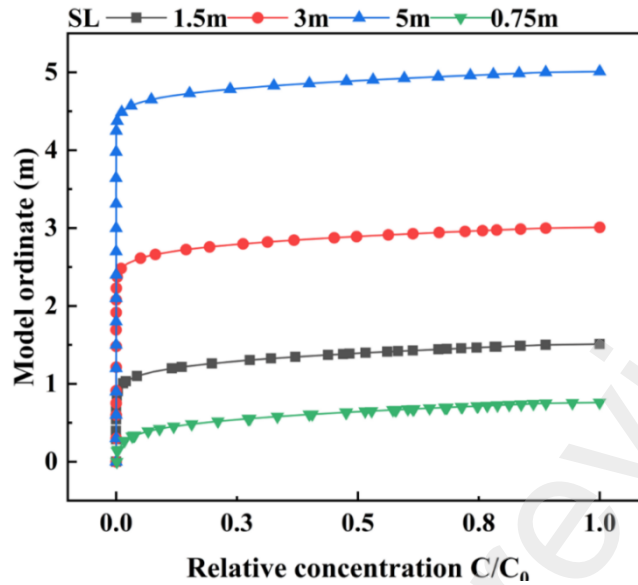
258 The thickness of the SL plays a crucial role in both the migration time of contaminants within
 259 the liner and the economic cost of the liner system. Understanding the appropriate thickness of the
 260 SL is therefore essential for the precise design of liner systems. To investigate this, SL thicknesses
 261 of 0.75 m, 1.5 m, 3 m, and 5 m were selected for further research and analysis.

262 As illustrated in [Fig.6](#), increasing the SL thickness from 0.75 m to 1.5 m does not significantly
 263 impact the concentration of contaminants near the GM. Instead, the concentration curve shifts
 264 upward, indicating an increase in the thickness at which the concentration becomes zero. However,
 265 as the SL thickness continues to increase beyond 1.5 m, the concentration of contaminants near the

266 GM remains relatively constant. For SL thicknesses of 0.75 m, 1.5 m, 3 m, and 5 m, the
267 concentrations are essentially identical, suggesting that the SL thickness does not significantly affect
268 the contaminant migration within the liner system.

269 These findings align with the work of [Pandey and Babu \(2017\)](#), who reported that contaminant
270 diffusion rates stabilize beyond a certain liner thickness due to the diminishing permeability and
271 adsorption capacity of the materials used. In contrast, [Brown and Thomas \(1998\)](#) found that for
272 highly volatile organic compounds, even slight increases in liner thickness could significantly
273 reduce diffusion rates, although their study focused on specialized industrial waste applications.
274 Additionally, economic analyses by [Sarkar et al. \(2016\)](#) suggest that the cost-benefit ratio becomes
275 unfavorable as SL thickness exceeds the optimal range, with increased material and construction
276 costs not justifying the marginal gains in containment efficacy. This economic perspective is crucial
277 for environmental engineering, where cost efficiency must be balanced with environmental
278 protection.

279 In practice, our results suggest that a standard SL thickness of 1.5 m is sufficient for typical
280 municipal waste containment. This recommendation supports sustainable design practices by
281 optimizing material use without compromising liner integrity or contaminant containment
282 capabilities.



283

284 **Fig. 6.** The variation of pollutant concentration with the thickness of SL at different depths of
 285 coordinates.

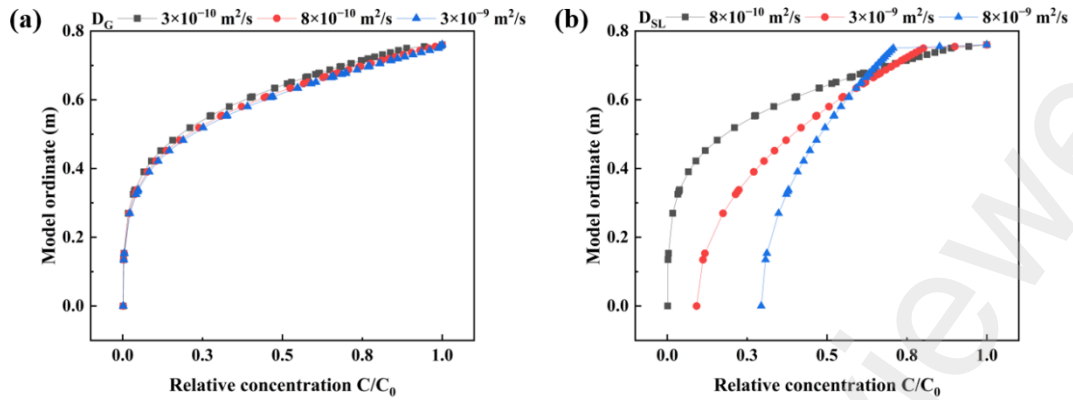
286 6.2 Diffusion coefficient

287 The diffusion coefficient is a pivotal factor in understanding contaminant migration within a
 288 liner, reflecting the varied material properties of GCL and SL. This study investigated the impacts
 289 of different diffusion coefficients for GCL and SL on contaminant dispersion. Specifically, diffusion
 290 coefficients for GCL were considered at $3 \times 10^{-10} \text{ m}^2/\text{s}$, $8 \times 10^{-10} \text{ m}^2/\text{s}$, and $3 \times 10^{-9} \text{ m}^2/\text{s}$; for SL, the
 291 coefficients were $8 \times 10^{-10} \text{ m}^2/\text{s}$, $3 \times 10^{-9} \text{ m}^2/\text{s}$, and $8 \times 10^{-9} \text{ m}^2/\text{s}$.

292 **Fig.7(a)** and (b) analyze the effects of these varying diffusion coefficients on contaminant
 293 migration within the composite liner. Additionally, **Fig.8** employs the COMSOL model to simulate
 294 pollutant concentrations, with sub-figures 8(a) to 8(c) highlighting the impacts of varying GCL
 295 diffusion coefficients, and sub-figures 8(d) to 8(f) showcasing those for SL. Variations in the GCL
 296 diffusion coefficient from $3 \times 10^{-10} \text{ m}^2/\text{s}$ to $3 \times 10^{-9} \text{ m}^2/\text{s}$ demonstrate a measurable influence on
 297 contaminant migration. The concentration profiles indicate that as the diffusion coefficient increases,
 298 the relative concentration of contaminants near the GM also increases. However, due to the

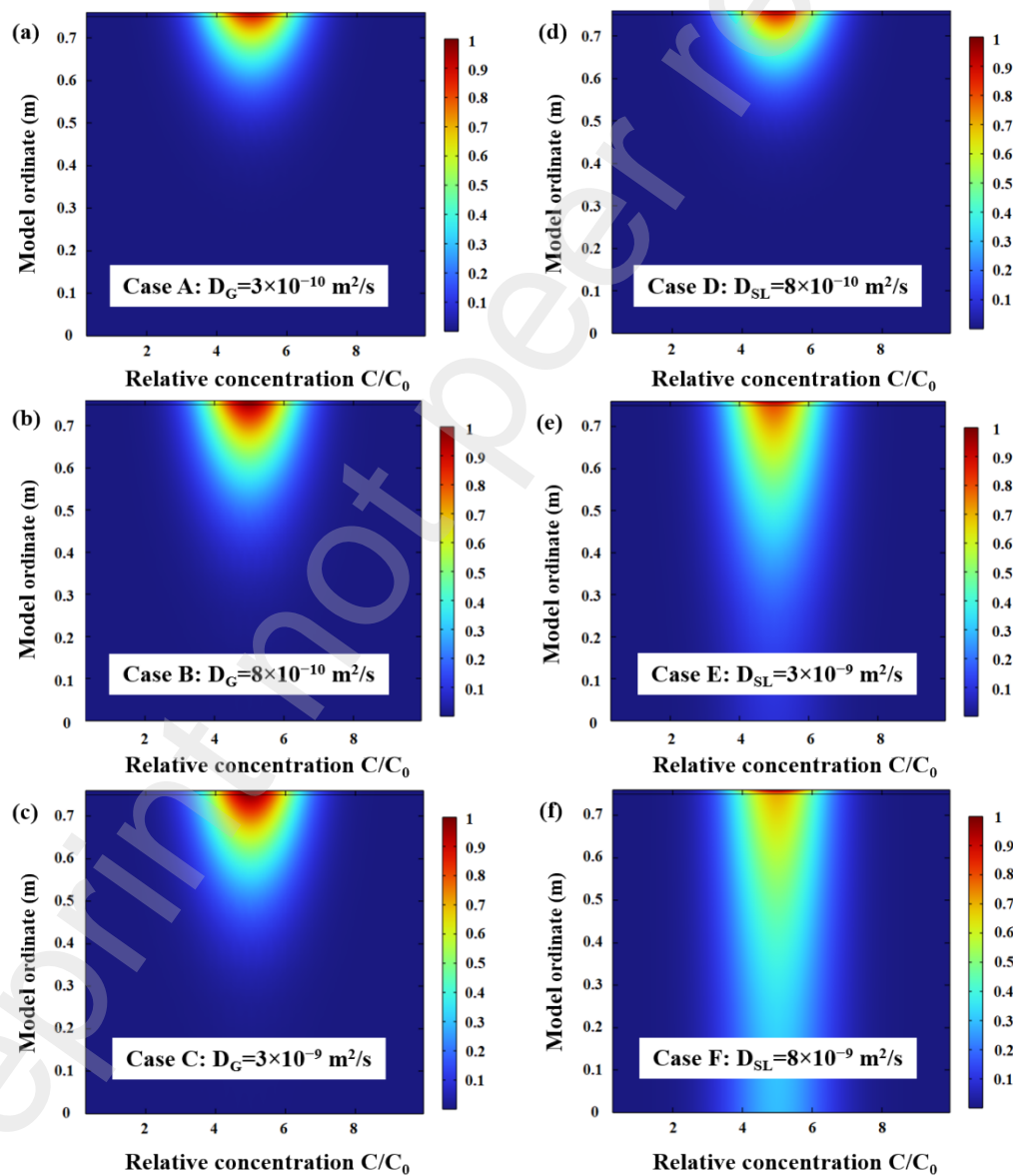
299 relatively thin nature of GCL layers, this impact remains moderate. The contour plots reveal steeper
300 concentration gradients with higher diffusion coefficients, indicating more rapid contaminant
301 migration through the GCL. Conversely, changes in the SL diffusion coefficient result in a more
302 pronounced increase in contaminant concentrations near the GCL interface. As the diffusion
303 coefficient of SL increases from $8 \times 10^{-10} \text{ m}^2/\text{s}$ to $8 \times 10^{-9} \text{ m}^2/\text{s}$, there is a significant increase in
304 the spread of contaminants. This is attributed to the greater thickness and permeability of the SL
305 compared to the GCL. The broader spread of contaminants with higher SL diffusion coefficients
306 underscores the stronger influence of SL on contaminant migration within the liner system.

307 [Xie et al. \(2013\)](#) found that increases in the diffusion coefficient in similar composite liners
308 lead to significantly enhanced migration rates of hydrophobic organic contaminants, particularly
309 when the liners exhibit higher permeability. Moreover, studies by [Anisimov et al. \(2020\)](#) further
310 corroborate that the material characteristics of SL can amplify the diffusion effects due to its greater
311 thickness and the interaction of multiple soil layers. Interestingly, the discrepancies between the
312 diffusion effects in GCL and SL highlighted in this study are also reflected in the work of [Majumder
313 et al. \(2023\)](#), who observed that diffusion in geosynthetic layers tends to stabilize more rapidly than
314 in soil layers, primarily due to the structured nature of geosynthetics compared to the heterogeneous
315 composition of soil. The results suggest that careful consideration of diffusion properties is essential
316 for designing effective composite liner systems. Optimizing the diffusion coefficients for both GCL
317 and SL can significantly enhance the containment performance of these systems.



318

319 **Fig. 7.** The variation of pollutant concentration with the diffusion coefficient at different depths of
 320 coordinates.



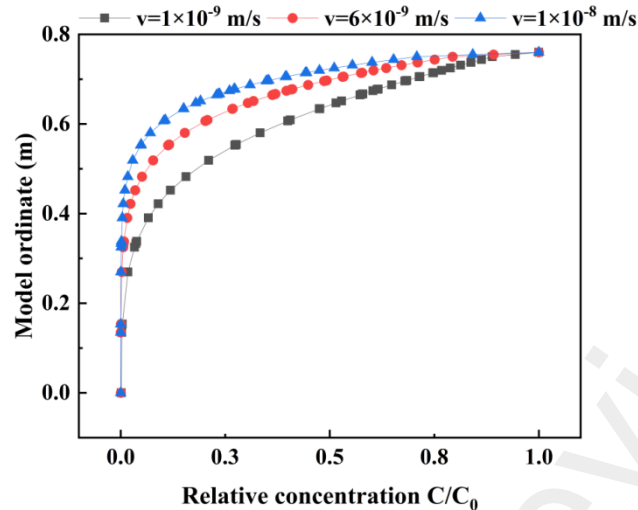
321

322 **Fig. 8.** Spatial distribution of pollutant concentration under diffusion coefficient:(a-c) diffusion
 323 coefficient of GCL;(d-f) diffusion coefficient of SL.

324 6.3 Convection coefficient

325 The convection process plays a pivotal role in contaminant transport within liner systems,
326 significantly impacting both GCL and SL layers. To elucidate the role of convection in contaminant
327 migration, convection coefficients of 1×10^{-9} m/s, 6×10^{-9} m/s, and 1×10^{-8} m/s were selected for
328 analysis.

329 [Fig.9](#) demonstrates that as the convection coefficient increases, the diffusion concentration of
330 contaminants gradually diminishes as contaminants penetrate deeper into the liner. Specifically,
331 [Fig.10\(a\)](#), [10\(b\)](#) and [10\(c\)](#) illustrate the effects of these varying convection coefficients as analyzed
332 using the COMSOL model. When the convection coefficient reaches 1×10^{-8} m/s, the ccontaminant
333 oncentration diminishes to approximately zero after migrating 0.3 m. Conversely, with a convection
334 coefficient of 1×10^{-9} m/s, the concentration decreases to zero after migrating 0.55 m. Clearly, the
335 convection coefficient significantly influences contaminant migration within the liner. Thus, in the
336 practical design of landfill projects, careful consideration of the convection coefficient is imperative
337 to ensure the rational adjustment of liner materials and design. [Yeo et al. \(2007\)](#) demonstrated that
338 higher convection coefficients significantly accelerate contaminant migration in synthetic liners due
339 to enhanced advection processes. Similarly, research by [Ameijeiras-Mariño et al. \(2017\)](#) in soil
340 liners found that increases in convection coefficients could reduce the residence time of
341 contaminants within the liner, potentially compromising the containment effectiveness unless
342 compensated by other design modifications. In practical applications, especially in landfill project
343 design, it is crucial to consider these convection coefficients to ensure the effective containment of
344 contaminants by making appropriate adjustments to liner materials and system designs.



345
 346 **Fig. 9.** The variation of pollutant concentration with the convection coefficient at different depths
 347 of coordinates.

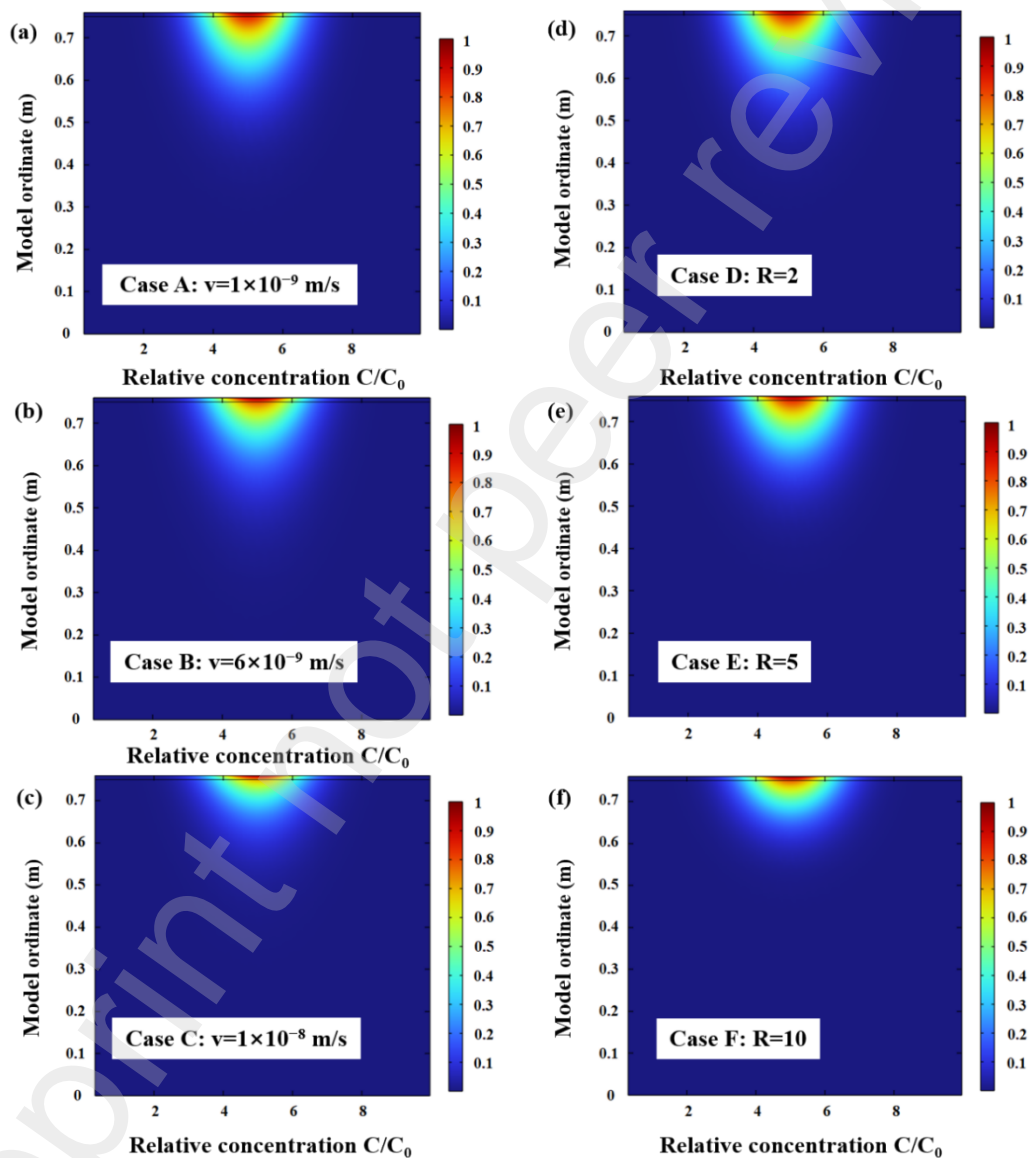
348 *6.4 Adsorption retardation factor*

349 The adsorption retardation factor has a certain effect on impeding the rapid migration of
 350 contaminants within the liner layer. Adsorption retardation factors of 2, 5, and 10 were employed
 351 to simulate contaminant migration of contaminants within the composite liner. Fig.10(d),10(e) and
 352 10(f) illustrate the effects of adsorption retardation factor as analyzed by COMSOL model.

353 Fig.11 demonstrates the impact of these differing adsorption retardation factor on contaminant
 354 migration. As the adsorption retardation factor increases, the migration of contaminants decelerates.
 355 For instance, with a retardation factor of 2, the contaminant concentration decreases to zero after
 356 migrating 0.25 m within the liner layer. When the retardation factor is increased to 5, the
 357 concentration drops to zero at 0.35 m. Furthermore, with a retardation factor of 10, the concentration
 358 reaches zero after migrating 0.55 m. This indicates that as the adsorption retardation factor increases,
 359 the migration of contaminants slow down, although the retarding effect on the contaminants
 360 decreases accordingly.

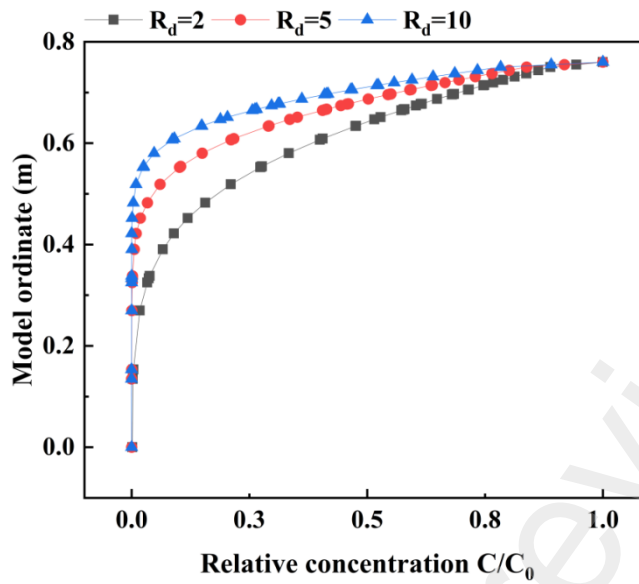
361 These findings align with the observations of Chrysikopoulos et al. (1990), who reported that

362 the sorption effect significantly slows down pollutant migration. Additionally, studies by Lin and
 363 Yeh (2020) corroborate that the larger the adsorption factor, the shorter the migration distance of
 364 pollutants. Therefore, if the adsorption retardation effect in the liner is significant, it is essential to
 365 incorporate the retardation factor into the mathematical model to accurately predict contaminant
 366 behavior.



367
 368 **Fig. 10.** Spatial distribution of pollutant concentration under convection coefficient and adsorption
 369 retardation factor: (a-c) convection coefficient; (d-f) retardation factor.

370



371
 372 **Fig. 11.** The variation of pollutant concentration with the adsorption retardation factor at different
 373 depths of coordinates.

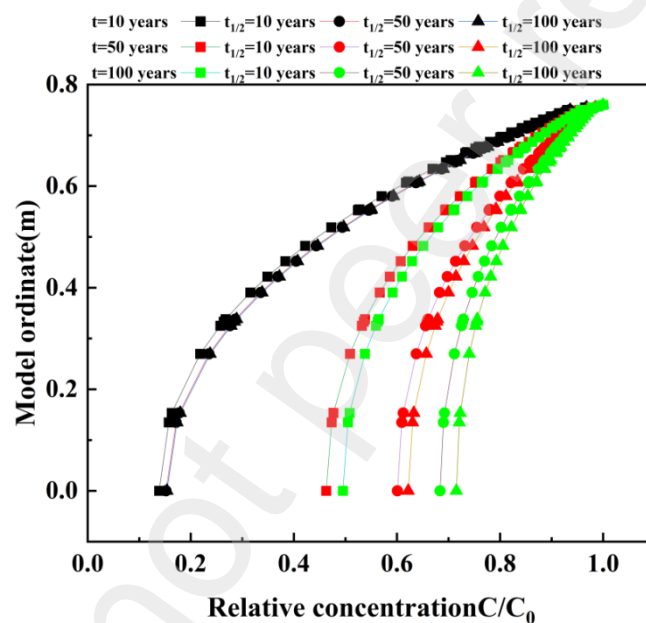
374 *6.5 Degradation coefficient*

375 [Fig.12](#) illustrates the effect of the degradation coefficient of organic pollutants, considering
 376 different half-lives set at 10 years, 50 years, and 100 years. The concentrations are compared for
 377 migration times of 10 years, 50 years, and 100 years.

378 When the migration time (t) is 10 years, the three concentration curves exhibit minimal
 379 differences. However, as the half-life decreases, the pollutant concentration also decreases. At $t =$
 380 50 years, significant differences between the concentration curves emerge, with the concentration
 381 under the 10-year half-life scenario notably lower than that under the 50-year and 100-year scenarios.
 382 The concentration is highest under the 100-year half-life scenario. As t increases to 100 years, these
 383 concentration differences become even more pronounced.

384 The results indicate that the half-life of organic pollutants in the composite liner system
 385 significantly affects the concentration of pollutants within the liner. However, due to the long
 386 degradation time and minimal degradation of organic pollutants over a short period, variations in
 387 degradation coefficients has a limited effect on preventing the migration of pollutants in the

388 composite liner. Feng et al. (2019a) and Peng et al. (2021), also proposed that when the half-life is
 389 short, the degradation effect is more pronounced. However, when the half-life is long, the
 390 degradation effect can be neglected in the short term. Understanding the degradation coefficients
 391 and their impact on pollutant migration is crucial for designing effective composite liner systems.
 392 While short-term degradation may not significantly influence pollutant concentration, long-term
 393 degradation can substantially reduce contaminant levels, enhancing the liner's protective
 394 performance.



395
 396 **Fig. 12.** The variation of pollutant concentration with the adsorption retardation factor at different
 397 depths of coordinates.

398 7. Limitations

399 One fundamental limitation of the proposed model in this study is its assumption of uniformity
 400 and isotropy within the same liner layer. This simplification overlooks the potential for
 401 heterogeneity and anisotropy, which are common in real-world scenarios. Additionally, the model
 402 does not account for the temporal changes in liner properties that can occur due to aging, chemical
 403 interactions with the leachate, or physical disturbances. Over time, the GM and other liner materials

404 can degrade or change their properties, which can alter the effectiveness of the containment system.
405 This temporal aspect is crucial for long-term assessments of landfill performance but is beyond the
406 scope of the current modeling approach.

407 Another limitation is the exclusion of macroscopic features such as cracks or joints within the
408 liner system, which can serve as preferential paths for the migration of contaminants. While the
409 model assumes a defective GM, it does not specifically simulate the complex flow dynamics that
410 can occur around these defects, nor does it consider the potential for repair or mitigation measures
411 that might be applied in practical settings.

412 **8. Summary**

413 Considering the uneven distribution of pollutants behind the GM in composite liners, a two-
414 dimensional model was developed to investigate the contaminant migration behavior. This model
415 accounts for convection, diffusion, adsorption, and degradation processes within the liner, and has
416 been validated through the one-dimensional analytical solution and the two-dimensional numerical
417 results computed using the COMSOL model. Analysis of key factors led to the following
418 conclusions:

419 (1) The concentration distributions of organic pollutants and metal pollutants in the liner differ to
420 some extent, and using the same function to describe these distributions can affect the extent of
421 contamination. Employing two distinct concentration distribution functions enhances accuracy.

422 (2) Compared to alternative analytical solutions and COMSOL validation results, the proposed
423 analytical solution demonstrates a satisfactory level of accuracy, effectively describing pollutant
424 migration processes in composite liners.

425 (3) The concentration curve of pollutants is more sensitive to changes in the diffusion coefficient of

426 SL than to changes in the diffusion coefficient of GCL. Specifically, as the diffusion coefficient of
427 SL increases from $8 \times 10^{-10} \text{ m}^2/\text{s}$ to $8 \times 10^{-9} \text{ m}^2/\text{s}$, the concentration curves intersect. However, when
428 the diffusion coefficient of GCL increases from $3 \times 10^{-10} \text{ m}^2/\text{s}$ to $3 \times 10^{-9} \text{ m}^2/\text{s}$, the concentration
429 distribution curve of pollutants exhibits minimal changes, indicating comparable pollution
430 prevention capabilities in both scenarios.

431 (4) Comparison results with the one-dimensional defective membrane GM/GCL/SL triple-layer
432 composite liners show that in the two-dimensional case, the accumulation rate of pollutants in the
433 liner slows down, the lateral pollutant range increases, and under the same conditions, it is more
434 difficult for pollutants to penetrate the composite liner layer.

435 **CRedit authorship contribution statement**

436 **Shan Zhao:** Conceptualization, Funding acquisition, Supervision, Writing – original draft, Writing
437 – review & editing. **Botao Sun:** Investigation, Methodology, Software, Writing –original draft.
438 **Xinjia Su:** Investigation, Formal analysis, Methodology.

439 **Declaration of Competing Interest**

440 The authors declare that they have no known competing financial interests or personal relationships
441 that could have appeared to influence the work reported in this paper.

442 **Data availability**

443 Data will be made available on request.

444 **Acknowledgments:** The author thanks the editor and anonymous reviewers for their valuable
445 comments on this manuscript. This study was financially supported by the National Natural Science
446 Foundation of China (No. 42477203, No. 42177129, No.41702241) and by China Postdoctoral
447 Science Foundation (No. 2022M720110).

448 References

- 449 Abiriga, D., Vestgarden, L.S., Klempe, H., 2020. Groundwater contamination from a municipal landfill: Effect of
450 age, landfill closure, and season on groundwater chemistry. *Sci. Total Environ.* 737, 140307.
451 <http://dx.doi.org/10.1016/j.scitotenv.2020.140307>
- 452 Ameijeiras-Mariño, Y., Opfergelt, S., Schoonejans, J., Vanacker, V., Sonnet, P., Jong, J., et al., 2017. Impact of low
453 denudation rates on soil chemical weathering intensity: A multiproxy approach. *Chem. Geol.* 456, 72-84.
454 <http://dx.doi.org/10.1016/j.chemgeo.2017.03.007>
- 455 Anisimov, V.S., Dikarev, D.V., Kochetkov, I.V., Ivanov, V.V., Anisimova, L.N., Tomson, A.V., et al., 2020. The
456 study of the combined effect of soil properties on the rate of diffusion of ⁶⁰Co. *Environ. Geochem. Health* 42,
457 4385-4398. <http://dx.doi.org/10.1007/s10653-020-00600-8>
- 458 Brown, K.W., Thomas, J.C., 1998. A comparison of the convective and diffusive flux of organic contaminants
459 through landfill liner systems. *Waste Manage. Res.* 16(3), 296-301.
- 460 Chrysikopoulos, C.V., Kitanidis, P.K., Robert, P.V., 1990. Analysis of One-Dimensional Solute Transport Through
461 Porous Media With Spatially Variable Retardation Factor. *Water Resour. Res.* 26, 437-446.
- 462 Ding, X., Feng, S., Zheng, Q., Peng, C., 2020. A two-dimensional analytical model for organic contaminants
463 transport in a transition layer-cutoff wall-aquifer system. *Comput. Geotech.* 128, 103816
464 <http://dx.doi.org/10.1016/j.compgeo.2020.103816>
- 465 Dominijanni, A., Manassero, M., 2021. Steady-state analysis of pollutant transport to assess landfill liner
466 performance. *Environ. Geotech.* 8, 480-494. <http://dx.doi.org/10.1680/jenge.19.00051>
- 467 Feng, S., Peng, M., Chen, H., Chen, Z., 2019a. Fully transient analytical solution for degradable organic contaminant
468 transport through GMB/GCL/AL composite liners. *Geotextiles and Geomembr.* 47, 282-294.
469 <http://dx.doi.org/10.1016/j.geotextmem.2019.01.017>
- 470 Feng, S., Peng, M., Chen, Z., Chen, H., 2019b. Transient analytical solution for one-dimensional transport of organic
471 contaminants through GM/GCL/SL composite liner. *Sci. Total Environ.* 650, 479-492.
472 <http://dx.doi.org/10.1016/j.scitotenv.2018.08.413>
- 473 Foose, G.J., Benson, C.H., Edil, T.B. 2002. Comparison of Solute Transport in Three Composite Liners. *J. Geotech.*
474 *Geoenviron. Engin.* 128(5): 391-403.
- 475 Ghosh, A., Kumar, S., Das, J., 2023. Impact of leachate and landfill gas on the ecosystem and health: Research trends
476 and the way forward towards sustainability. *J Environ. Manage.* 336, 117708.
477 <https://doi.org/10.1016/j.jenvman.2023.117708>
- 478 Gómez-García, R., Campos, D. A., Aguilar, C. N., Madureira, A.R., Pintado, M., 2021. Valorisation of food agro-
479 industrial by-products: From the past to the present and perspectives. *J. Environ. Manage.* 299, 113571.
480 <https://doi.org/10.1016/j.jenvman.2021.113571>
- 481 Lin, Y., Yeh, H., 2020. A simple analytical solution for organic contaminant diffusion through a geomembrane to
482 unsaturated soil liner: Considering the sorption effect and Robin-type boundary. *J. Hydrol.* 586,124873.
483 <http://dx.doi.org/10.1016/j.jhydrol.2020.124873>
- 484 Ling, X., Chen, W., Schollbach, K., Brouwers, H. J. H., 2024. Low permeability sealing materials based on sewage,
485 digestate and incineration industrial by-products in the final landfill cover system. *Constr. Build. Mater.* 412,
486 134889. <https://doi.org/10.1016/j.conbuildmat.2024.134889>
- 487 Majumder, M., Venkatraman, S., Bheda, M., Patil, M., 2023. Numerical Studies on the Performance of Geosynthetic
488 Reinforced Soil Walls Filled with Marginal Soil. *Indian Geotech. J.* 53, 805-826.
489 <http://dx.doi.org/10.1007/s40098-022-00706-z>
- 490 Nanda, S., Berruti, F., 2021. Municipal solid waste management and landfilling technologies: a review[J]. *Environ.*
491 *Chem. Lett.* 19(2), 1433-1456.

492 Pandey, M.R., Babu, G.S., 2017. Effects of compaction and initial degree of saturation on contaminant transport
493 through barrier. *PanAm. Unsaturated Soils*, pp, 168-176.

494 Peng, C., Feng, S., Chen, H., Ding, X., Yang, C., 2021. An analytical model for one-dimensional diffusion of
495 degradable contaminant through a composite geomembrane cut-off wall. *J. Contam. Hydrol.* 242, 103845.
496 <http://dx.doi.org/10.1016/j.jconhyd.2021.103845>

497 Pu, H., Qiu, J., Zhang, R., Zheng, J., 2019. Analytical solutions for organic contaminant diffusion in triple-layer
498 composite liner system considering the effect of degradation. *Acta. Geotech.* 15, 907-921.
499 <http://dx.doi.org/10.1007/s11440-019-00783-0>

500 Qian, Y., Hu, P., Lang-Yona, N., Xu, M., Guo, C., Gu, J.D., 2024. Global landfill leachate characteristics:
501 Occurrences and abundances of environmental contaminants and the microbiome[J]. *J. Hazard. Mater.* 461,
502 132446. <https://doi.org/10.1016/j.jhazmat.2023.132446>

503 Rouholahnejad, E., Sadrnejad, S.A., 2009. Numerical simulation of leachate transport into the groundwater at landfill
504 sites. *Proc.18th. World IMACS/MODSIM Congr. Cairns, Australia.* pp, 13-17.

505 Rowe, R. K., Hamdan, S., 2020. Performance of GCLs after long-term wet–dry cycles under a defect in GMB in a
506 landfill. *Geosynth. Int.* 30(3), 225-246. <https://doi.org/10.1680/jgein.21.00023a>

507 Rowe, R. K., Reinert, J., Li, Y., Awad, R., 2023. The need to consider the service life of all components of a modern
508 MSW landfill liner system. *Waste. Manage.* 161, 43-51. <https://doi.org/10.1016/j.wasman.2023.02.004>

509 Sarkar, R., Daalia, A., Narang, K., Garg, S., Agarwal, P., Mudgal, A., 2016. Cost Effectiveness of flexible pavement
510 on stabilised expansive soils. *Int. J. Geomate.* 10(1), 1595-1599.

511 Shu, S., Zhu, W., Shi, J., 2019. A new simplified method to calculate breakthrough time of municipal solid waste
512 landfill liners. *J. Cleaner Prod.* 219, 649-654. <http://dx.doi.org/10.1016/j.jclepro.2019.02.050>

513 Sobral, B., Samper, J., Montenegro, L., Mon, A., Guadaño, J., Gómez, J., et al., 2024. 2D model of groundwater
514 flow and total dissolved HCH transport through the Gállego alluvial aquifer downstream the Sardas landfill
515 (Huesca, Spain). *J. Contam. Hydrol.* 265, 104370. <http://dx.doi.org/10.1016/j.jconhyd.2024.104370>

516 Sun, X., Xu, Y., Liu, Y., Nai, C., Dong, L., Liu, J., et al., 2019. Evolution of geomembrane degradation and defects
517 in a landfill: Impacts on long-term leachate leakage and groundwater quality. *J. Cleaner Prod.* 224, 335-345.
518 <https://doi.org/10.1016/j.jclepro.2019.03.200>

519 Sun, D., Li, T., Peng, M., Wang, L., Chen, Z., 2022. Semi-analytical solution for the two-dimensional transport of
520 organic contaminant through geomembrane with strip defects to the underlying soil liner. *Int. J. Numer. Anal.*
521 *Methods Geomech.* 47, 392-409. <http://dx.doi.org/10.1002/nag.3474>

522 Teng, C., Zhou, K., Peng, C., Chen, W., 2021. Characterization and treatment of landfill leachate: A review. *Water.*
523 *Res.* 203, 117525. <http://dx.doi.org/10.1016/j.watres.2021.117525>

524 Touze-Foltz, N., Xie, H., Stoltz, G., 2021. Performance issues of barrier systems for landfills: A review. *Geotextiles*
525 *and Geomembr.* 49, 475-488. <http://dx.doi.org/10.1016/j.geotextmem.2020.10.016>

526 Trauger, R., Tewes, K., 2020. Design and installation of a state-of-the-art landfill liner system[M]//*Geosynthetic*
527 *Clay Liners.* CRC Press. pp, 175-181.

528 Wijekoon, P., Koliyabandara, P.A., Cooray, A.T., Lam, S.S., Athapattu, B.C.L., Vithanage, M., 2022. Progress and
529 prospects in mitigation of landfill leachate pollution: Risk, pollution potential, treatment and challenges. *J.*
530 *Hazard. Mater.* 421, 126627. <http://dx.doi.org/10.1016/j.jhazmat.2021.126627>

531 Woodman, N. D., Rees-White, T. C., Beaven, R. P., Stringfellow, A. M., Barker, J. A., 2017. Doublet tracer tests to
532 determine the contaminant flushing properties of a municipal solid waste landfill[J]. *J. Contam. Hydrol.* 203, 38-
533 50. <https://doi.org/10.1016/j.jconhyd.2017.05.008>

534 Wu, X., Shi, J., He, J., 2015. Rule of diffusion of organic pollutants through GCL + AL liners considering
535 biodegradation (in Chinese). *J. Hohai. Univ (Nat. Sci.).* 43(01),16-21.

- 536 Wu, L., Zhan, L., Lan, J., Chen, Y., Zhang, S., Li, J., et al., 2021. Leachate migration investigation at an unlined
537 landfill located in granite region using borehole groundwater TDS profiles. *Eng. Geol.* 292, 106259.
538 <https://doi.org/10.1016/j.enggeo.2021.106259>
- 539 Xie, H., Cai, P., Yan, H., Zhu, X., Thomas, H.R., Chen, Y., et al. 2023. Analytical model for contaminants transport
540 in triple composite liners with depth-dependent adsorption process. *J. Hydrol.* 625, 130162.
541 <http://dx.doi.org/10.1016/j.jhydrol.2023.130162>
- 542 Xie, H., Chen, Y., Lou, Z., 2010. An analytical solution to contaminant transport through composite liners with
543 geomembrane defects. *Sci. China. Technol. Sci.* 53, 1424-1433. <http://dx.doi.org/10.1007/s11431-010-0111-7>
- 544 Xie, H., Jiang, Y., Zhang, C., Feng, S., 2014. An analytical model for volatile organic compound transport through
545 a composite liner consisting of a geomembrane, a GCL, and a soil liner. *Environ. Sci. Pollut. Res.* 22, 2824-
546 2836. <http://dx.doi.org/10.1007/s11356-014-3565-5>
- 547 Xie, H., Thomas, H.R., Chen, Y., Sedighi, M., Zhan, T.L., Tang, X., 2013. Diffusion of organic contaminants in
548 triple-layer composite liners: an analytical modeling approach. *Acta. Geotech.* 10, 255-262.
549 <http://dx.doi.org/10.1007/s11440-013-0262-3>
- 550 Yeo, K.H., Zhou, T., Leong, K.C., 2007. Experimental Study of Passive Heat Transfer Enhancement in a Drag-
551 Reducing Flow. *Heat Transfer Eng.* 28: 9-18. <http://dx.doi.org/10.1080/01457630600985501>
- 552 Yu, C., Liu, J., Ma, J., Yu, X., 2018. Study on transport and transformation of contaminant through layered soil with
553 large deformation. *Environ. Sci. Pollut. Res.* 25, 12764-12779. <http://dx.doi.org/10.1007/s11356-018-1325-7>
- 554 Zhang, J., Zhang, J., Xing, B., Liu, G., Liang, Y., 2021. Study on the effect of municipal solid landfills on
555 groundwater by combining the models of variable leakage rate, leachate concentration, and contaminant solute
556 transport. *J. Environ. Manage.* 292, 112815. <https://doi.org/10.1016/j.jenvman.2021.112815>
- 557